Nuclear Inst. and Methods in Physics Research, A 1039 (2022) 167014

Contents lists available at ScienceDirect

Nuclear Inst. and Methods in Physics Research, A

journal homepage: www.elsevier.com/locate/nima

Upgrade of the OSIRIS primary spectrometer

A. Perrichon, F. Demmel *

ISIS Facility, Rutherford Appleton Laboratory, Didcot, OX11 0QX, United Kingdom

ARTICLE INFO

Keywords:
Neutron spectrometer
Monte Carlo simulation
Supermirror guide

ABSTRACT

A proposed upgrade is presented for the primary part of the indirect time-of-flight near-backscattering spectrometer OSIRIS at the ISIS Facility. This upgrade comprises a new supermirror guide with non-linear defocusing and focusing sections, a new wavelength bandwidth chopper system and a flexible slit system to adjust the divergence. The new neutron guide has an elliptical defocusing section, a curved section and an elliptical focusing section. The estimated gain factor in intensity is wavelength dependent between 4 and 7 at the sample position with a homogeneous divergence distribution on a smaller beam spot. The divergence will increase by up to a factor 3 compared to the present guide, but can be reduced by up to a factor 5 through the slit system. The increased guide cross section requires a system of two counter-rotating disc choppers with larger disc diameters than the present ones for the selection of the wavelength bandwidth. Estimates for the performance indicate that the proposed upgrade will keep the OSIRIS spectrometer competitive in the years to come.

1. Introduction

The OSIRIS spectrometer at the ISIS Facility, UK, has seen its first neutrons in the year 1997. At that time, it went into operation as a cold neutron diffractometer and a few years later the spectrometer capabilities were installed and commissioned [1–5]. This indirect spectrometer is based on the concept of analyzing the band of incoming energies through the time-of-flight and the final fixed energy through Bragg scattering from a near backscattering crystal analyzer.

One of the first instruments of this type was the IRIS spectrometer at the ISIS Facility, UK [6,7]. It exploits a cooled pyrolytic graphite analyzer in a near-backscattering geometry. This geometry resulted at that time in a relaxed energy resolution of about 15 μeV combined with a large dynamic range. Backscattering spectrometers at reactor sources achieve a much higher energy resolution (≈ 1 μeV) with a concomitant smaller dynamic range [8–10]. To increase the restricted dynamic range of backscattering instruments at continuous sources time-of-flight options have been proposed and implemented [11–14]. On pulsed sources new developments aimed to increase the energy resolution towards μeV resolution with the combination of silicon analyzers and short pulses [15–17].

Compared to the IRIS spectrometer OSIRIS achieved a gain in intensity by using a supermirror guide and a larger analyzer unit [5]. Further improvements were made with the installation of a movable Beryllium filter to remove the second order reflection of the pyrolytic graphite analyzer [18]. The energy resolution and lineshape have successfully been modeled with Monte Carlo simulations [19], which laid the foundations for further developments. To enhance the performance of the instrument with respect to energy resolution and allow novel challenging studies of, for instance, slow diffusive motions of ions in battery materials, an upgrade is under way to implement a Si(111) analyzer unit with an energy resolution of $\Delta E \approx 10$ μeV [20,21]. The improved energy resolution with the Si(111) analyzer will consequently reduce the measured intensity and hence the primary upgrade will deliver a welcome compensation for the intensity loss due to the better energy resolution. The current OSIRIS guide, constructed in the mid-nineties of the last century, is a straight $m = 2$ supermirror guide with a $m = 3.6$ linear focusing section at the end, where m stands for m-times the critical angle of total reflection of a natural-Ni coated guide. At that time this guide was state-of-the-art. Cold neutrons around 6 Å can have up to 9 reflections in the 32 m long $m = 2$ supermirror guide until the end of the guide. Due to the finite reflectivity at the $m = 2$ edge the large number of reflections limits the transmission of the divergent neutrons decisively in such a straight guide [22]. This is the cause for the quite modest gain factor in flux of about 1.6 at $\lambda \approx 6$ Å for OSIRIS in comparison with the natural Ni guide on IRIS [5].

Schanzer et al. demonstrated that a ballistic guide with an elliptic focusing section has a much superior performance compared to a straight guide or a linear focusing guide [23]. New guide geometries have less reflections and can transport cold neutrons very effectively over long distances [24,25]. The performance of these novel guide geometries has been assessed in the past, see for example [26–30], and the elliptic geometry emerged as the most favorable one. High transmission values of 80% have been simulated for cold neutrons over

* Corresponding author.
E-mail address: franz.demmel@stfc.ac.uk (F. Demmel).

https://doi.org/10.1016/j.nima.2022.167014
Received 28 March 2022; Received in revised form 13 May 2022; Accepted 31 May 2022
Available online 21 June 2022

distances much longer than the 32 m guide on OSIRIS [25]. Therefore, a new guide with an elliptic geometry has been proposed to replace the present OSIRIS guide [20]. Furthermore, the elliptic geometry allows to focus neutrons on a smaller sample size, a necessity when it comes to investigate small sample quantities of, for example, biological samples or single crystals. As a consequence of the increased flux an increase in divergence must be accepted, which is not a concern for most of the QENS experiments. To provide a tool to reduce the divergence, e.g. for low energy dispersive spin excitations, a slit system will be integrated. With the increase of the guide dimensions an upgrade of the bandwidth chopper system becomes necessary and therefore the whole primary spectrometer will be modernized. A first account for a new guide was reported in [31]. Here we present a comprehensive study for the upgrade of the whole primary spectrometer and compare its potential performance with similar spectrometers in the world.

Constraints and simulations

The present guide is curved with a radius of $R = 2050$ m to avoid direct line-of-sight and has a constant cross section of 43×65 mm^2 before it converges to 22×44 mm^2 with a $m = 3.6$ straight focusing section. The distance between the guide end and the sample position is 250 mm. The characteristic wavelength λ_c, where the transmitted intensity drops to 67%, is related to the guide width $a = 43$ mm and curvature radius R according to [32]:

$$\lambda_c = \sqrt{\frac{\pi}{Nb}}\sqrt{\frac{2a}{R}} = \frac{2\pi}{k_\perp}\sqrt{\frac{2a}{R}} \tag{1}$$

with the purely material-dependent maximum vertical wave vector $k_\perp = m\sqrt{4\pi Nb} = m \cdot 0.0109$ Å^{-1} for a supermirror guide with a m-value coating. Nb denotes the coherent scattering length density of the total reflecting material, which is in this case natural Nickel. The critical angle for total reflection of neutrons with a wavelength λ for a supermirror is $\theta_c = 0.1 \cdot m \cdot \lambda$ in degrees. Therefore, the $m = 3.6$ focusing section will provide a maximum divergence of about 4° for the present guide around the standard wavelength range of $\lambda \approx 6$ Å. For the $m = 2$ guide at OSIRIS, Eq. (1) results in a characteristic wavelength of $\lambda_c = 1.92$ Å.

For the design of the new primary spectrometer, a few requirements need to be obeyed. The secondary spectrometer will remain at its position and, hence, a curved section will be introduced which shifts the initial flight path of the neutrons at the sample position by 186 mm. The length from moderator to sample (34.00 m) is fixed and also the length from moderator to guide entrance (1.70 m). The guide will end at a distance of 250 mm before the sample. Furthermore, the curved section is to be designed in such a way that the direct line-of-sight ends at least 2 m before the end of the guide. The direct line-of-sight L for a curved guide is related to the width a and curvature radius R in the following way [33]: $L = \sqrt{8aR}$. That condition influences the possible width of the guide in combination with the curvature radius. The beam shutter is shared with the neighboring IRIS spectrometer and this shared access limits the maximum width of the new guide at the beginning. The direction of both instruments is then separated by an angle of 1.7° and thus after the beginning of the guide a defocusing section can be implemented without interference with the neighboring guide. The optimization of the guide height needs to consider the increase in opening and closing times for the slow rotating bandwidth choppers. A maximum limit of the guide height of 200 mm was set, which still allows to implement a chopper system with the same performance as the present system. The guide system has been optimized for maximum intensity on two typical sample sizes: 20×30 mm^2 and 10×10 mm^2. The intensity gain is nurtured from the novel geometry with less reflections and an increased divergence.

For the optimization of the guide Monte Carlo simulations were performed using the McStas ray-tracing package [34–36], automated with an in-house Matlab code. The first McStas component characterizes the ISIS source seen through the 25 K hydrogen moderator leading to OSIRIS, which is described in the external moderator file *TS1verBase2016_LH8020_newVM-var_North06_Iris* produced by the ISIS Neutronics group. This file assumes a 80 % para-hydrogen concentration in the hydrogen moderator. For the optimization we utilized a cold neutron wavelength band with energies of 1.4 − 4.0 meV, corresponding to $\lambda = 4.5$–7.6 Å. This wavelength band is used in most of the QENS and low-energy spectroscopy studies on OSIRIS. A further energy band around 10–20 meV was utilized for some additional simulations.

The guide is described by a list of vertices and faces, each with individual m-values, produced by Matlab and read in by the *Guide_anyshape_r* component. Given the choice of elliptically-shaped defocusing and focusing sections and the constraints on the maximum guide dimensions, dimensions at guide entrance and line-of-sight suppression, the number of degrees of freedom of the guide geometry is limited. They are the length of the defocusing and focusing elliptic sections and the vertical and horizontal focal point positions by the sample. More details can be found in a technical report [37].

The *Guide_anyshape_r* was modified to use the same reflectivity model as the other McStas component [36], i.e. a model defined by a maximum reflectivity at low-angle of $R_0 = 0.99$, the critical scattering vector $Q_c = 0.0219$ Å^{-1}, the width of supermirror cut-off $W = 1/300$ Å^{-1} and the slope of reflectivity α, which corresponds to the linear decrease in reflectivity with increasing reflection wave vector beyond $m = 1$. For the current OSIRIS guide, a value of $\alpha = 6.07$ Å is used, which corresponds to the performance in reflectivity achieved at the time of construction. For the new supermirror guide, recent developments in guide fabrication technology were taken into account. Therefore reflectivities of 80%, 72% and 63% at the $m = 4$, $m = 5$ and $m = 6$ edges were assumed [38], which correspond to $\alpha \approx 3.5$ Å. The slit system was incorporated directly in the file describing the guide using neutron absorbing faces. Neutron rays are stored individually at the moderator surface and upon reaching the sample position, using *monitor_nD* components. The spatial distribution and divergence of the neutron beam as well as quantities such as the gain factor in intensity and the Brilliance transfer (BT) are computed in post-processing with Matlab.

Once the guide geometry was determined we optimized the guide coating. The maximum gain factor achievable with a uniform $m = 6$ coating was used as reference. The m-values of the guide were decreased from $m = 6$ to $m = 3$, in sections from the guide entrance and exit, for the top and bottom walls, inner walls and outer walls individually. Intensity losses are monitored until an intensity decrease of 1% is reached.

Finally, we performed analytical calculations of the chopper system, which consists of two bandwidth choppers. Due to space constraints both chopper axis are located to the side of the guide. With the increased height of the guide counter-rotating double disc choppers are considered to achieve the required opening and closing times. Each chopper is characterized by its diameter and z-position along the guide. The angular opening of the choppers are calculated to maximize the dynamic window for a configuration of OSIRIS with the PG002 analyzer with a 50 Hz repetition rate of the neutron source. The position of the second chopper is optimized to minimize the amount of unfiltered long-wavelength neutrons reaching the sample. This is calculated via the transmission of the time–wavelength neutron distribution from the moderator, which can pass through the chopper system.

2. Results and discussion

The best performing design is shown in Fig. 1. It has a 10.0 m long elliptic defocusing section, followed by a 15.35 m long straight curved section and finishes with a 6.7 m long elliptically shaped focusing section. The curved section has a curvature radius of 1208 m and a maximum guide width of 81 mm. The line-of-sight ends 2.2 m from the guide end. The dimensions at guide entrance are 47×90 mm^2, in the curved section 81×200 mm^2 and at the guide end 28×50 mm^2. The

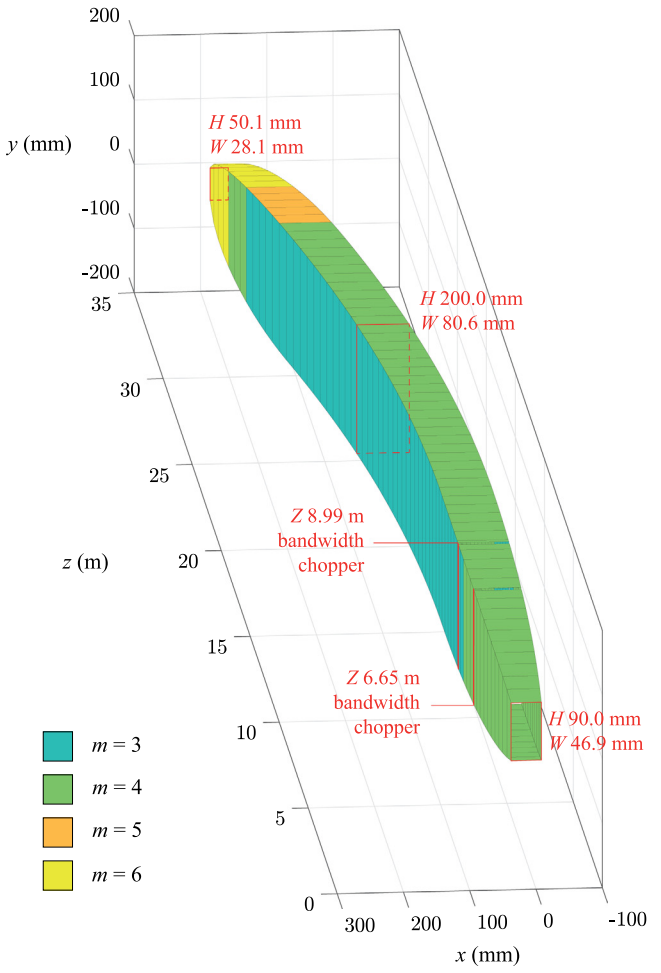

Fig. 1. A 3D schematic picture of the new optimized guide is presented. Included are the guide dimensions at the begin, middle part and at the end. The colors indicate the coating of the supermirror guide. The positions of the two bandwidth choppers are also included.

focal points at the moderator are determined by the guide dimensions, resulting in a vertical focal point at about 50 cm in front of the moderator and a horizontal focal point about 60 cm behind it. The focal points of the focusing ellipse are 3 cm before and 20 cm after the sample for the vertical and horizontal ellipses. The deviations of the focal points from exactly on the moderator and sample positions are due to the extended source and sample dimensions of 120×120 mm^2 and up to 20×30 mm^2, respectively.

The spatial distribution of the neutrons at the sample position is shown in Fig. 2(a), together with the two sample dimensions indicated as white rectangles. The spatial distribution is better focused than the present one, which has an approximate 20×40 mm^2 beam spot size [31]. The divergence profiles for the two sample dimensions are shown in Fig. 2(b) and (c). The divergences (FWHM) are about 8.0° vertically and 4.7° horizontally for the 20×30 mm^2 sample and about 10.4° vertically and 5.3° horizontally for the 10×10 mm^2 sample. This is in contrast to the existing instrument, which has divergences of about 3° vertically and horizontally [37]. Due to the vertically increased divergence of a factor 3 and horizontally by a factor 1.5 we can expect intensity gain factors around 5.

Note that we have also evaluated alternative geometries. Guide geometries with parabolic defocusing and focusing sections and all combinations of parabolic and elliptic sections were investigated. Additionally, we also considered a setup with two ellipses inclined against each other, instead of using a curved section, to achieve the deviation

Table 1
The optimized m-values are presented for all sections of the guide from moderator to sample.

Section	Length	m-value (outer)	m-value (inner)	m-value (top/bottom)
Defocusing	6.0	4	4	4
Defocusing	4.0	3	3	4
Curved	15.35	4	3	4
Focusing	1.2	3	3	4
Focusing	2.5	3	3	5
Focusing	1.5	4	4	6
Focusing	1.5	6	6	6

from the direct line- of-sight. However, all these other geometries did not achieve the gain factors of the elliptic/curved/elliptic design. Furthermore, some of them showed an inhomogeneous divergence distribution at the sample position.

Then the m-coating profile of the guide was optimized and the results are reported in Table 1. In the final design only quite short sections of $m = 5$ and $m = 6$ coating are required. For the first defocusing section, which is nearest to the target and moderator, a maximum m-value of $m = 4$ was imposed for coating stability reasons. This restriction was chosen to avoid on the long term any reduction of reflectivity due to potential radiation damage for a high-m coating. The simulation predicted only a small gain if that section would be covered with a larger m-value coating. To achieve a low value of the characteristic wavelength in the curved section, a higher m-value ($m = 4$ outer) will be used in this part of the guide. Compared to the current guide, the curved section of the new guide has a smaller radius ($R = 1208$ m), an increased width ($a = 81$ mm) and a coating of $m = 4$. According to Eq. (1) we get $\lambda_c \approx 1.7$ Å. This characteristic wavelength will allow to use the Si(333) reflection in the future.

To assess more precisely the performance of the guide system we calculated the brilliance transfer (BT) from the moderator to the sample position, which is a measure of how well the guide transports neutrons of a certain divergence and wavelength. It is calculated as the ratio of the brilliance, defined as the $number\ of\ neutrons/\mathrm{s}/\mathrm{cm}^2/\mathrm{sr}/\text{Å}$ at the sample and moderator positions using two monitors of identical size. According to Liouville's theorem BT cannot exceed 1. In Fig. 3 we plot the calculated BT for a band of cold neutrons (1.4–4.0 meV) for the 2 sample sizes dependent on the divergence (circles and diamonds). Included are also the brilliance transfer values for the present guide (crosses and squares). It demonstrates that cold neutrons with a wide range of divergence are transported highly effectively from the moderator to the sample position. The BT reaches more than 75% over a wide range of divergence up to ±3°. The increase in transmission over the present guide contributes to the intensity gain and confirms the optimal geometry of the design.

Fig. 4 shows the intensity gain factors at the sample position as a function of wavelength for the two different sample dimensions. Gain factors are defined as the ratio between the intensities simulated for the new guide design and the present guide on OSIRIS. With the new optimized guide intensity gains between 4 and 7 are expected. The actual gain factor could be larger by up to a factor of 2, because these values do not include potential aging effects of the present guide. At SINQ, PSI, the guide system has been replaced recently. The previous guide to the CAMEA instrument has a similar length and design as the present OSIRIS guide and was installed at the same time. After installation of a new elliptic shaped supermirror guide a gain factor of 6 has been reported for this beam line [39]. Even though the exact details of the geometry are different, this result grants confidence that the new guide on OSIRIS will achieve the proposed substantial gain factors.

The increased flux with this new guide design comes with an increased divergence, as can be seen by inspecting Fig. 2. For some experiments, for example the measurement of single crystal dispersive

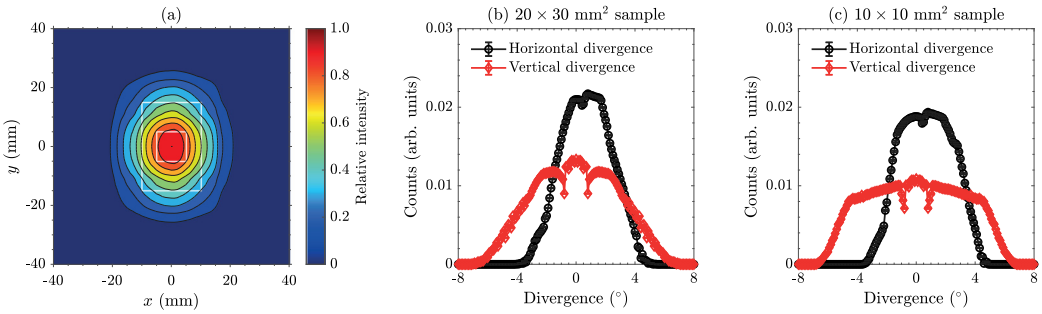

Fig. 2. In panel (a) a PSD-picture of the spatial distribution of the neutrons at the sample position is plotted. The rectangle indicates the sample dimensions for the optimization. Panels (b) and (c) show the horizontal and vertical divergence of the cold neutron beam at the sample position for the two sample dimensions.

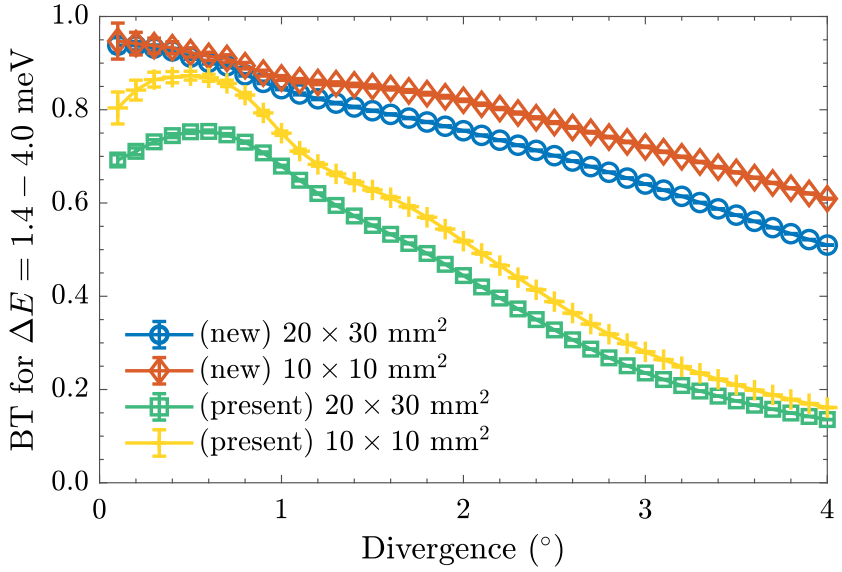

Fig. 3. The brilliance transfers for the new (circles and diamonds) and present guide (squares and crosses) are plotted for the two sample dimensions dependent on the divergence (HWHM-values).

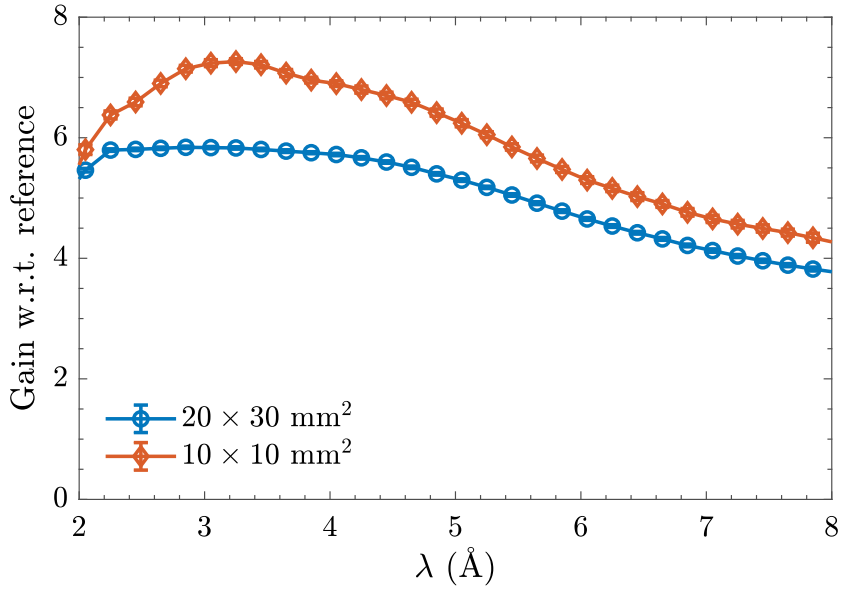

Fig. 4. Intensity gain factors of the new guide as a function of neutron wavelength λ are plotted for the two sample dimensions.

excitations, there might be a need to restrict the divergence. In addition, with the new silicon analyzer the vertical wave vector direction can be analyzed with the help of position sensitive detectors. In order to limit the divergence a slit system consisting of three flexible slits in the focusing part of the guide has been included. Such an approach has been successfully used in the WISH diffractometer at the ISIS Facility [40]. The installation of a slit system also might be beneficial for background reduction. An optimization has been done based on long

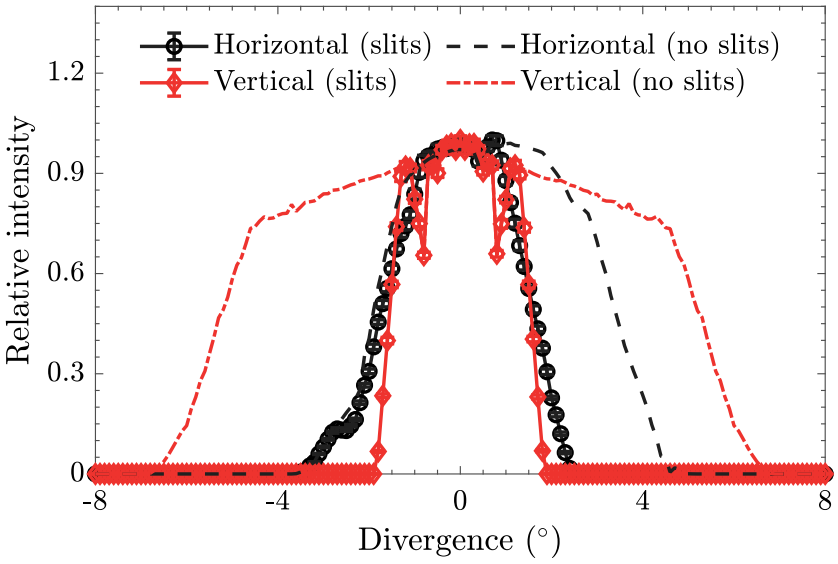

Fig. 5. The divergence at sample position with a three-slit system is plotted in comparison with the divergence of the unrestricted setup. Note that the off-centered distribution of the horizontal divergence due to the curved guide is compensated using asymmetric slit openings.

wavelength neutrons. One slit will be placed at the end of the guide and the other two slits in a distance of 10 cm and 80 cm from the guide exit. Fig. 5 shows the divergence distributions in a slit configuration which will reduce the divergence to FWHM = 3° horizontally and vertically. The divergence distribution looks fairly homogeneous and, using an asymmetric opening of the horizontal slits, the horizontal divergence can be centered. A price on intensity has to be paid for this divergence reduction with an intensity loss that brings the gain factor back to 1. This is fully consistent as the present guide has a divergence of about 3°. Further simulations have shown that the divergence can be reduced to 2°, if needed.

Concomitant with the increased flux transported to the spectrometer there is a risk to increase the background. Even though the power of the source remains on the same level the opening up of the guide dimensions might release more fast neutrons towards the sample. For this reason we decided to keep the sample position out of direct-line-of-sight and we therefore anticipate no noise increase from fast neutrons. Furthermore, the new introduced slit system, which sits near the sample position, will reduce the background from thermal neutrons and one could expect even a smaller background level in the spectrometer compared to the present configuration without such a slit system.

To accommodate the new guide design two new bandwidth choppers will need to be incorporated. With the increase of the guide dimensions the opening and closing times of the bandwidth choppers will increase and will reduce the available dynamic range. At the 6 m chopper position the height of the guide will increase by a factor 3. A different positioning of the choppers above or below the guide is not possible due to interference with the neighboring IRIS beamline. There are different possibilities to mitigate the problem with the opening and closing times.

A focusing section from the shutter to the first chopper position could be used to reduce the guide height at the chopper position. We investigated with Monte Carlo simulations a design with an elliptic or parabolic focusing section and afterwards an adapted elliptic curved guide to the sample position. All optimization efforts resulted in a loss of intensity of about 20%–30% in the cold wavelength range. The amount of losses would reduce the performance of the upgrade distinctly and alternative options should be considered. Another solution would be to install a disc with a larger diameter to retain the opening and closing times. With a guide height increase of a factor 3 the disc diameter would have to increase to about 1.8 m. Such a large disc would interfere with the shielding of the neighboring beamline and it became apparent that at that position only a maximum disc diameter of about 1.2 m is technically feasible, which again is a not an ideal solution. The third option is to replace the single discs with counter-rotating double disc choppers (DDC). With a modest increase of the diameter from 600 mm to 810 mm the required opening and closing times can then be achieved. Therefore, a system of 2 double disc choppers is the preferred option.

To investigate the performance of the DDC system space–time calculations for the transmitted neutrons have been performed. There exists a possibility that slow neutrons emerge from the moderator which find a path through the chopper opening and reach the sample in the next pulse frame. The aim is to optimize the positioning of the two DDC with regard to the suppression of these unwanted slow neutrons. A limit of slow neutron wavelength of 40 Å was set, which is to be compared with the value of 32 Å for the current chopper system. The spectral flux $\Phi(v)dv$ from a moderator with a Maxwell–Boltzmann velocity distribution is the number of neutrons through the unit area per second with velocities between v and $v + dv$ and may be given by [41]: $\Phi(v)dv \propto v^3 exp(-mv^2/2k_BT)dv$ with T the moderator temperature. This relation transforms in wavelength to a $1/\lambda^5$ decrease towards long wavelengths and hence neutrons of $\lambda \geq 40$ Å emerging from the moderator are reduced by more than 4 orders of magnitude compared to the number of neutrons at the final neutron wavelength of around 6 Å. These slow neutrons would need to be up-scattered at the sample by about 1.8 meV to reach the detector through the analyzer. All low temperature experiments would not allow these processes due to the detailed balance condition. At high temperatures the scattering probability would be a product of the reduced small amount of long wavelength neutrons with the value of the scattering function at the energy transfer of around 1.8 meV. For practically all measurements the probability that these slow neutrons could reach a detector is far below the noise to signal ratio of the spectrometer, which is about 10^{-4} [19].

The optimal solution for two DDC is positioning them in a distance from the moderator of 6.65 m and 8.99 m. While the first chopper diameter will be 810 mm the second disc diameter has to be increased to 870 mm to compensate for the increased guide height at its position in order to achieve the same opening times of 0.78 ms at 50 Hz for the two choppers. For this case we obtain open angles on the chopper discs of 77.4° and 95.2° for the first and second chopper. At the sample position the sum of the opening and closing times amounts to 5.7 ms, which is 28.5% of the total available time frame. The transmission plateau corresponds to a symmetric dynamic range of 1.85 ± 0.44 meV

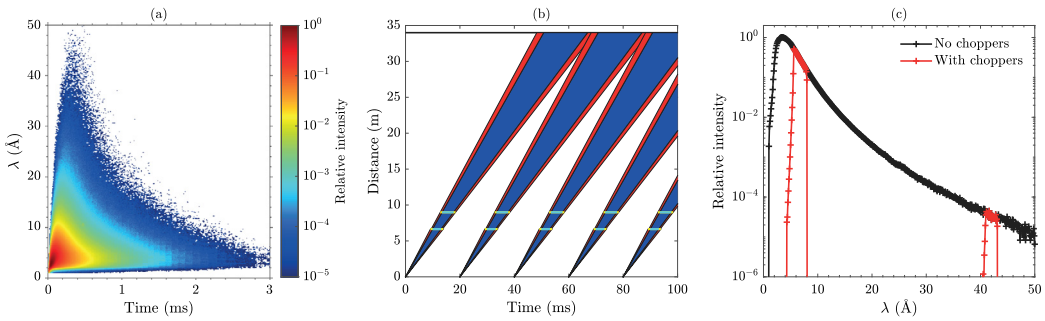

Fig. 6. Panel (a) shows the wavelength–time distribution of neutrons on a logarithmic intensity scale, back-propagated from the sample position to the moderator surface. Panel (b) shows a time–distance diagram for the transmission of cold neutrons in the PG002 setting. The red areas depict the opening and closing time frames. Panel (c) shows the transmitted range of wavelength bands.

(corresponding to a wavelength range of $\lambda = 6$ Å to $\lambda = 7.6$ Å) for PG002 at 50 Hz. The plateau value is a good measure for the available dynamic range, even though the practically usable dynamic range extends into the opening and closing range. Because of its position further downstream it is the second chopper that defines the opening and closing times at the sample position. This fact provides an opportunity to extend the dynamic range by increasing the disc diameter of the second chopper, which would be technically possible. Increasing the diameter to 1000 mm reduces the opening time to 0.67 ms. Note that this increase does not modify the open angle of the second chopper of 95.2°, because of the fixed 20 ms time frame. However, the transmission plateau increases to a slightly larger dynamic range of ±0.46 meV. Another possibility to improve the dynamic range is to introduce a degree of overlap of the closing time of a pulse with the opening time of the next pulse, which effectively increases the length of the transmission plateau at the price of being unable to exploit the time region of overlap. For a 50% overlap of opening and closing times, which corresponds to 2.55 ms at the sample position, the open angle on the chopper discs would be 84.9° for the first chopper and 101.3° for the second chopper. This leads to a dynamic range of ±0.5 meV. Both options add only a modest amount in dynamic range to the transmission plateau and the first option appears to be the preferred choice.

Fig. 6 panel (a) shows a color map in logarithmic scale of the time–wavelength distribution of neutrons emerging from the moderator. It is calculated by back-propagating the neutrons from the sample position to the moderator. In this way, the impact of the guide on the neutron transmission is included and only neutrons that actually reach the sample are considered. Panel (b) shows the time–distance diagram for a 50 Hz PG002 setting, where the blue area is the fully useful dynamic range and the red area is the time range associated with opening and closing of the choppers. Note that the opening and closing times are here 50% overlapping. In panel (c) the wavelength dependent spectrum is plotted on a logarithmic scale for the non-chopped case and with the choppers operating. In contrast to the time–distance diagram, which considers a point source in time, Fig. 6(c) takes the full distribution in time of the pulses into account for neutrons generated up to 3 ms, the entire range of Fig. 6(a). Only a wavelength band around 42 Å can pass the choppers. The intensity is reduced by about 4 orders of magnitude between the exploited range and the unwanted neutron bandwidth. For the PG004 setting the unwanted neutron bandwidth is around 39 Å, for the Si(111) configuration around 42 Å and for the 25 Hz settings the wavelength band is beyond 50 Å.

Finally we want to consider the performance of the upgraded OSIRIS instrument in comparison with similar TOF-backscattering spectrometers. The wavelength dependent flux at the sample position of the present guide has been determined some time ago as $\Phi(\lambda) = 3 \times 10^6$ $n/\mathrm{cm}^2/\mathrm{s}/\text{Å}$ for $\lambda = 6$ Å [5]. With a gain factor of around 5 a spectral flux of $\Phi(\lambda) \approx 1.5 \times 10^7$ $\mathrm{n/cm^2/s/Å}$ can be expected. Just now an upgrade of the target and moderator system is under way on target station 1 of the ISIS Facility. The installation of a new hydrogen moderator with a water pre-moderator will increase the flux of cold neutrons by about a factor 2 [42]. Hence a spectral flux of $\Phi(\lambda = 6\ \text{Å}) \approx 3 \times 10^7$ $\mathrm{n/cm^2/s/Å}$ can be looked forward to for OSIRIS. For the BASIS spectrometer at the SNS, Oak Ridge, a flux of $\Phi = 1.3 \cdot 10^7$ $\mathrm{n/cm^2/s}$ with a wavelength band of $\Delta\lambda = 0.5$ Å around $\lambda = 6.4$ Å at a source power of 0.5 MW was reported [16]. With the now achieved full source power of 1.4 MW at SNS the flux on the upgraded OSIRIS spectrometer will be similar to BASIS, keeping in mind that the resolution on the BASIS instrument ($\Delta E = 3.5$ μeV) is much better than on OSIRIS now ($\Delta E = 25$ μeV). With the new silicon analyzer the energy resolution on OSIRIS will improve to $\Delta E \approx 10$ μeV [21] and the resolution gap to BASIS will be reduced. Although the improved energy resolution with the Si(111) analyzer might indicate a reduction of the measured intensity compared to the graphite analyzer, simulations predicted a similar measured intensity due to an increased solid angle and no need for the utilization of a Beryllium filter [21]. Therefore one can expect that the primary upgrade intensity gain will also benefit the silicon analyzer configuration fully. For the Miracles instrument at the ESS, Sweden, intensity gain factors between 5 and 10 were predicted compared to the BASIS instrument for a similar resolution, when the ESS has reached full power of 5 MW [43,44]. Until the ESS reaches its full capabilities OSIRIS will remain a highly competitive cold neutron backscattering spectrometer on an international level.

3. Conclusions

After 25 years of operation and several improvements on the secondary spectrometer, it is timely for an upgrade of the whole primary spectrometer of the OSIRIS instrument. A new guide with a hybrid design combining non-linear defocusing and focusing sections with a curved guide between emerged as the optimal solution. The new supermirror guide will have elliptic defocusing and focusing sections and will deliver intensity gain factors of 4–7 on the sample position. Concomitant to the gain in intensity the divergence will increase accordingly by up to a factor 3. As a flexible tool to adjust the divergence a slit system will be integrated into the guide. The geometric dimensions of the guide will increase significantly and consequently the single disc wavelength band chopper system will be replaced by a counter-rotating double-disc system. The substantial increase in flux will keep the OSIRIS spectrometer competitive in comparison with instruments at sources with higher power. The primary spectrometer upgrade will ensure a bright future for OSIRIS and the user community it serves beyond the year 2030.

Declaration of competing interest

The authors declare that they have no known competing financial interests or personal relationships that could have appeared to influence the work reported in this paper.

Acknowledgments

This work was supported by the Science and Technology Facilities Council (STFC), United Kingdom. Numerous discussions with the ISIS Engineering team are gratefully acknowledged.

References

[1] D. Martin y Marero, S. Campbell, C.J. Carlile, J. Phys. Soc. Japan 65 (1996) 245.
[2] D. Martin y Marero, D. Engberg, Physica B 267–268 (1999) 134.
[3] D. Martin y Marero, Appl. Phys. A Mater. Sci. 74 (2002) S289.
[4] K.H. Andersen, D. Martin y Marero, D. Barlow, Appl. Phys. A Mater. Sci. 74 (2002) S237.
[5] M.T.F. Telling, K.H. Andersen, Phys. Chem. Chem. Phys. 7 (2005) 1255; T.F. M.Telling, S.I. Campbell, D. Engberg, D. Martin, y. Marero, K.H. Andersen, Phys. Chem. Chem. Phys. 18 (2016) 8243.
[6] C.J. Carlile, M.A. Adams, Physica B 182 (1992) 431.
[7] C.J. Carlile, M.A. Adams, P.S.R. Krishna, M. Prager, K. Shibata, P. Westerhuijs, Nucl. Instrum. Methods A 338 (1994) 78.
[8] B. Frick, E. Mamontov, L. van Eijck, T. Seydel, Zeit. Phys. Chem. 224 (2010) 33.
[9] A. Meyer, R.M. Dimeo, P.M. Gehring, D.A. Neumann, Rev. Sci. Instrum. 74 (2003) 2759.
[10] O. Kirstein, M. Prager, D. Richter, Appl. Phys. A Mater. Sci. 74 (2002) S133; J. Wuttke, A. Budwig, M. Drochner, H. Kämmerling, J. F.-Kayser, H. Kleines, V. Ossovyi, L.C. Pardo, M. Prager, D. Richter, G.J. Schneider, H. Schneider, S. Staringer, Rev. Sci. Instrum. 83 (2012) 075109.
[11] F. Demmel, Ph. Bernhard, A. Magerl, E. Steichele, Physica B 276-278 (2000) 116.
[12] P. Tregenna-Piggott, F. Juranyi, P. Allenbach, Neutron News 19 (2008) 20.
[13] L. van Eijck, L. Gerard, B. Frick, T. Seydel, H. Schober, Nucl. Instrum. Methods A 672 (2012) 64.
[14] M. Appel, B. Frick, A. Magerl, Sci. Rep. 8 (2018) 13580.
[15] F. Demmel, K.H. Andersen, Meas. Sci. Tech. 19 (2008) 034021.
[16] E. Mamontov, K.W. Herwig, Rev. Sci. Instrum. 82 (2011) 085109.
[17] N. Takahashi, K. Shibata, T.J. Sato, Y. Kawakita, I. Tsukushi, N. Metoki, K. Nakajima, M. Arai, Nucl. Instrum. Methods A 600 (2009) 91; K. Shibata, N. Takahashi, Y. Kawakita, M. Matsuura, T. Yamada, T. Tominaga, W. Kambara, M. Kobayashi, Y. Inamura, T. Nakatani, K. Nakajima, M. Arai, Jpn. Phys. Soc. Conf. Proc. 8 (2015) 036022.
[18] F. Demmel, D. McPhail, J. Crawford, D. Maxwell, K. Pokhilchuk, V. Garcia-Sakai, S. Mukhopadyay, M.T.F. Telling, F.J. Bermejo, N.T. Skipper, F. Fernandez-Alonso, EPJ Web Conf. 83 (2015) 03003.
[19] F. Demmel, K. Pokhilchuk, Nucl. Instrum. Methods A 767 (2014) 426.
[20] F. Demmel D. McPhail, C. French, D. Maxwell, S. Harrison, J. Boxall, N. Rhodes, S. Mukhopadhyay, I. Silverwood, V. Garcia Sakai, F. Fernandez-Alonso, J. Phys. Conf. Ser. 1021 (2018) 012027.
[21] A. Perrichon, F. Fernandez-Alonso, M. Wolff, M. Karlsson, F. Demmel, Nucl. Instrum. Methods A 947 (2019) 162740.
[22] P. Böni, F. Grünauer, C. Schanzer, Nucl. Instrum. Methods A 624 (2010) 162.
[23] C. Schanzer, P. Böni, U. Filges, T. Hils, Nucl. Instrum. Methods A 529 (2004) 63.
[24] P. Böni, Nucl. Instrum. Methods A 586 (2008) 1.
[25] K.H. Kleno, K. Lieutenant, K.H. Andersen, K. Lefmann, Nucl. Instrum. Methods A 696 (2012) 75.
[26] C. Pelley, F. Kargl, V. Garcia Sakai, M. Telling, F. Fernandez-Alonso, F. Demmel, J. Phys.: Conf. Ser. 251 (2010) 012063.
[27] H. Jacobsen, K. Lieutenant, C. Zendler, K. Lefmann, Nucl. Instrum. Methods A 717 (2013) 69.
[28] C. Zendler, D. Nekrassov, K. Lieutenant, Nucl. Instrum. Methods A 746 (2014) 39.
[29] S. Weichselbaumer, G. Brandl, R. Georgii, J. Stahn, T. Panzner, P. Böni, Nucl. Instrum. Methods A 793 (2015) 75.
[30] D.M. Rodriguez, D.D. DiJulio, P.M. Bentley, Nucl. Instrum. Methods A 808 (2016) 101.
[31] A. Perrichon, F. Fernandez-Alonso, M. Wolff, M. Karlsson, F. Demmel, J. Surf. Investig.: X-Ray Synchrotron Neutron Techn. 14 (2020) S169.
[32] A. Dianoux, G. Lander (Eds.), Neutron Data Booklet, Institut Laue Langevin, Grenoble, 2002.
[33] B.T.M. Willis, C.J. Carlile, Experimental Neutron Scattering, Oxford University Press, Oxford, 2009.
[34] K. Lefmann, K. Nielsen, Neutron News 10 (1999) 20.
[35] P. Willendrup, E. Fahri, K. Lefmann, Physica B 350 (2004) E735.
[36] P. Willendrup, K. Lefmann, J. Neutron Res. 23 (2021) 7.
[37] A. Perrichon, F. Demmel, Technical Report TR RAL 2020 002, 2020.
[38] C. Schanzer, M. Schneider, P. Böni, J. Phys. Conf. Ser. 746 (2016) 012024.
[39] T. Geue, F. Juranyi, Chr. Niedermayer, J. Kohlbrecher, J. Stahn, U. Gasser, M. Yamada, Chr. Klauser, M. Kenzelmann, Chr. Rüegg, U. Filges, Neutron News 32 (2021) 37.
[40] L.C. Chapon, P. Manuel, P.G. Radaelli, C. Benson, L. Perrott, S. Ansell, N. Rhodes, D. Raspino, D. Duxbury, E. Spill, J. Norris, Neutron News 22 (2011) 22.
[41] G.L. Squires, Introduction To the Theory of Thermal Neutron Scattering, Cambridge University Press, 1978.
[42] G. Skoro, S. Lilley, R. Bewley, Physica B 551 (2018) 381.
[43] N. Tsapatsaris, P.K. Willendrup, R.E. Lechner, H.N. Bordallo, EPJ Web Conf. 83 (2015) 03015.
[44] N. Tsapatsaris, R.E. Lechner, M. Markó, H.N. Bordallo, Rev. Sci. Instrum. 87 (2016) 085118.